Published in final edited form as:
*Biomaterials*. 2014 February ; 35(7): 2089–2096. doi:10.1016/j.biomaterials.2013.11.040.

# Optical imaging of fibrin deposition to elucidate participation of mast cells in foreign body responses

**Yi-Ting Tsai**[#a], **Jun Zhou**[#a], **Hong Weng**[a], **Ewin N. Tang**[a], **David W. Baker**[a], and **Liping Tang**[a,b,*]

[a] Department of Bioengineering, University of Texas at Arlington, Arlington, TX 76019, USA

[b] Department of Biomedical Science and Environmental Biology, Kaohsiung Medical University, Kaohsiung 807, Taiwan

[#] These authors contributed equally to this work.

## Abstract

Mast cell activation has been shown to be an initiator and a key determinant of foreign body reactions. However, there is no non-invasive method that can quantify the degree of implant-associated mast cell activation. Taking advantage of the fact that fibrin deposition is a hallmark of mast cell activation around biomaterial implants, a near infrared probe was fabricated to have high affinity to fibrin. Subsequent *in vitro* testing confirmed that this probe has high affinity to fibrin. Using a subcutaneous particle implantation model, we found significant accumulation of fibrin-affinity probes at the implant sites as early as 15 min following particle implantation. The accumulation of fibrin-affinity probes at the implantation sites could also be substantially reduced if anti-coagulant – heparin was administered at the implant sites. Further studies have shown that subcutaneous administration of mast cell activator – compound 48/80 – prompted the accumulation of fibrin-affinity probes. However, implant-associated fibrin-affinity probe accumulation was substantially reduced in mice with mast cell deficiency. The results show that our fibrin-affinity probes may serve as a powerful tool to monitor and measure the extent of biomaterial-mediated fibrin deposition and mast cell activation *in vivo*.

### Keywords

*In vivo* imaging; Near infrared fluorescence; Fibrin; Biomaterial; Inflammation; Biocompatibility

## 1. Introduction

Fibrinogen/fibrin accumulation at the implant sites has been shown to be critical in triggering foreign body reactions, including coagulation, inflammation (such as heart attack, ischemic stroke, and pulmonary embolism) and infection [1–4]. Since fibrin is a ligand for CD54 (ICAM-1), CD11b/CD18 (CR3, Mac-1) and CD11c/CD18 (CR4, p150/95), adhesion-promoting receptors expressed by endothelial cells, neutrophils, monocytes/macrophages, as well as subsets of dendritic, natural killer, and T cells, localized fibrin deposition is thought to be responsible for localized immune cell recruitment [5–7]. In addition, the interaction of



* Corresponding author. Department of Bioengineering, University of Texas at Arlington, P.O. Box 19138, Arlington, TX 76019-0138, USA. Tel.: +1 817 272 6075; fax: +1 817 272 2251. ltang@uta.edu (L. Tang)..

Appendix A. Supplementary data

Supplementary data related to this article can be found at http://dx.doi.org/10.1016/j.biomaterials.2013.11.040.

Mac-1(CD11b/CD18) and fibrin formation could trigger the production and release of inflammatory chemokines, such as tumor necrosis factor-alpha (TNF-α) and interleukin-1β (IL-1β), by inflammatory cells [8,9]. Since numerous studies have showed that inflammatory diseases, such as glomerulonephritis, lung ischemia, and rheumatoid arthritis, are substantially alleviated with fibrin depletion, it is possible that fibrin-mediated immune responses are critical to the pathogenesis of many inflammatory diseases [10].

Many cells and processes might contribute to localized fibrin deposition and consecutive edema formation [11]. Substantial evidences support the pivotal role played by mast cells in the initiation of edema and fibrin deposition of many inflammatory diseases, including cutaneous anaphylaxis, antigen-induced arthritis, and also reverse passive arthus reaction [12]. In addition, our previous studies suggest that mast cell activation (degranulation with histamine release) is mainly responsible for acute/chronic inflammatory responses to biomaterial implants [4,13–15]. These results suggest that the monitoring of mast cell activation-mediated fibrin deposition at the implant site may serve as an early indicator of foreign body reactions.

Currently, histology is a commonly-used method to determine fibrin deposition in tissue. However, histological methods cannot be used to continuously monitor the inflammatory processes without multiple biopsies or sacrificing many animals. In addition, preparation and analysis of tissue samples is very tedious and time-consuming. Therefore, a new method is needed to evaluate fibrin deposition surrounding biomaterial implants. *In vivo* imaging has emerged as a promising technique due to its ability to detect and evaluate fibrin deposition in inflammation and tumor lesions in a continuous, non-invasive, real-time manner. Several imaging methods have been developed to detect fibrin deposition in inflammation and tumor sites [16,17]. Specifically, EP-1873, a short fibrin-specific peptide conjugated with four Gd-DTPA units, exhibited the selective enhancement of ruptured atherosclerotic plaques in a rabbit model [18]. An improved version of this probe, EP-2104R, replaced the Gd-DTPA groups with a more stable Gd-DOTA chelator for MR signal enhancement [19]. The EP-2104R probe has been used to evaluate arterial and chamber clots. A Mn-based nanoparticle decorated with fibrin-specific monoclonal antibodies has been fabricated and its T1-weighted MR images of *in vitro* clots showed a significant contrast enhancement [20]. Recently, fluorescent dye-labeled cross-linked iron oxide (CLIO) nanoparticles functionalized with FXIII-specific peptide (GNQEQVSPLTLLKC) and fibrin(ogen) targeting peptide (GPRPPGGSKGC) have been prepared for *in vitro* detection of clots by both MR and optical imaging modalities [17]. However, none of these probes have been investigated for their ability to detect fibrin deposition surrounding biomaterial implants. In addition, the potential role of mast cell activation on fibrin deposition around biomaterials has yet to be determined.

In the present study, an NIR fibrin probe is developed to monitor the accumulation of fibrin in the biomaterial implantation site. NIR fluorescence is selected mainly due to low cost, high sensitivity, reduction of absorption and scattering of the photons by the tissues and elimination of auto-fluorescence signal [21]. Fibrin-affinity peptide (GPRPPGGSKGC) was chosen due to its highly avid fibrinaffinity ability and high resistance to proteolysis [22–24]. The efficacy of fibrin-affinity probes in recognizing fibrin deposition was studied *in vitro*. Using an *in vivo* imaging system, we further assessed the effectiveness of such fibrin-affinity probes in quantifying the extent of biomaterial implant-mediated fibrin deposition. The influence of mast cell activation on fibrin accumulation was then determined using mast cell-deficient WBB6F1-W/W$^{v}$ (W/W$^{v}$) mice and their normal littermates.

## 2. Materials and methods

### 2.1. Materials

Peptide (GPRPPGGSKGC with amide of C terminal, purity >98%) was purchased from Pi Proteomics, LLC (Huntsville, AL). Near infrared dye-Oyster®-800 TFP Ester (Oyster-800) was acquired from Boca Scientific Inc (Boca Raton, FL). $TiO_2$ (5–10 nm in diameter) and $SiO_2$ (30 nm in diameter) were obtained from Sun Innovations, Inc. (Fremont, CA). Poly lactic acid (PLA) was purchased from DURECT Co. (Birmingham, AL).

### 2.2. Preparation of fibrin-affinity probe

The fibrin-affinity probe was prepared by directly conjugating peptides with Oyster800 following the manufacturer's protocol from BOCA Scientific. In brief, peptide (GPRPPGGSKGC, 5.5 mg/mL in PBS) was incubated with Oyster800 dye (1 mg/mL in PBS) overnight at pH 8.0 and 4 °C. The fibrin-affinity probe was purified by exhausting dialysis against deionized water. The probe was then lyophilized (yield: 61%) and stored at –20 °C for further use.

### 2.3. Optical property of fibrin-affinity probes

The optical properties and bioactivities of the fibrin probe were characterized. Absorbance and fluorescence spectra of the fibrin-affinity probes were measured using a UV–Vis spectrophotometer (Lambda 19 Spectrometer, PerkinElmer, MA) and a fluorescence spectrometer (Shimadzu RF-5301PC, Japan), respectively. The cytotoxicity of the fibrin-affinity probes was then determined using 3T3 fibroblasts and an MTS assay as described earlier [25].

### 2.4. In vitro fibrin binding tests

Fibrin-coated glass beads were produced by incubating all glass beads with 200 mL fibrinogen (4000 mg/mL in isotonic PBS; 50 mM sodium phosphate plus 100 mM NaCl, pH 7.4) in individual wells of a 48-well plate. Following the addition of fibrinogen, 0.5 mL (1 U/mL) thrombin was added to each well to generate a homogeneous fibrin coating on glass beads. Surface fibrin was then allowed to fully polymerize at 37 °C for 5 min [4]. The glass beads were then transferred to new wells for the probe binding tests. For that, a 100 μL of fibrin-binging probes (GPRPPGGSKGC-Oyster800) or its control (Oyster800) (10 μg/mL) was added to the wells and incubated at 37 °C for 1 h. The supernatant on the glass beads was removed and then washed three times to remove unbound probes from the glass beads. Fluorescence intensities of glass beads were measured using a Tecan Infinite M 200 plate reader (San Jose, CA) at emission of 830 nm (excitation at 760 nm).

### 2.5. In vivo inflammation models

Female Balb/c mice (20–25 g), purchased from Taconic Farms (Germantown, NY), were used in this investigation. The animal experiments were approved by the University of Texas at Arlington Animal Care and Use Committee (IACUC). We evaluated the specificity of the fibrin probes by administering thrombin in the subcutaneous space. To test the efficacy of the fibrin-affinity probes in targeting fibrin formation, 25 U thrombin was injected subcutaneously as described earlier [26]. To induce localized inflammatory responses, 10 mg $TiO_2$ was implanted into various locations on the back of mice. To investigate the effects of time, 60 μL of fibrin-affinity probe solution (0.5 mg/mL) was administered via retro-orbital injection after $TiO_2$ implantation. The fluorescence intensities surrounding $TiO_2$ implants were recorded at different time points. To determine the role of mast cell activation on fibrin deposition, mice were subcutaneously injected with 100 μg of c48/80, a mast cell activator, or saline. To trigger varying extents of inflammatory responses

in the same animals, 10 mg of $TiO_2$, $SiO_2$ and PLA particles were used as control subjects to trigger various degrees of foreign body reactions. PLA particles (5–10 μm in diameter) were synthesized as previously demonstrated [27]. Finally, to investigate the role of mast cells in the biomaterial inflammatory response, mast cell-deficient WBB6F1-W/$W^v$ (W/$W^v$) mice and their normal littermates, WBB6F1-+/+ (+/+) were used. Different particles, $TiO_2$, $SiO_2$ and PLA, were implanted into both mice. Following particle implantation, 60 μL of fibrin-affinity probe solution (0.5 mg/mL) was administered via retro-orbital injection. Whole body images of mice were taken using Carestream In vivo FX Pro (f-stop: 2.5, excitation filter: 760 nm, emissions filter: 830 nm, 4 × 4 binning; Carestream Health, Rochester, NY). After background correction, regions of interests (ROIs) were drawn over the implantation locations, and the mean fluorescence intensities for all pixels in the fluorescent images were calculated using Carestream Molecular Imaging Software, Network Edition 4.5 (Carestream Health).

### 2.6. Immunohistochemical evaluation of biomaterial-mediated tissue responses

At the end of the studies, the test animals were sacrificed and the implantation sites/inflamed tissues were isolated for histological analyses. All tissues underwent cryosectioning followed by Hematoxylin–Eosin (H&E) and fibrin staining. All histological sections were imaged under a Leica DMLB microscope (Leica, Wetzlar, Germany) equipped with a QImaging Retiga Exi 1394 digital CCD camera (QImaging, Surrey, British Columbia, Canada). Quantitative histological analysis of the total numbers of inflammatory cells throughout the implantation sites was performed using NIH ImageJ [27,28]. The relative amount of fibrin (area covered by fibrin) was determined from IHC slices via a pre-determined threshold and the total thresholding area calculated using NIH ImageJ [29].

### 2.7. Statistical analyses

All the results were expressed as mean ± standard error of the mean (SEM). One-way analysis of variance (ANOVA) and student *t*-test were performed to compare the difference between groups. A value of $p \leq 0.05$ was considered to be significant.

## 3. Results

### 3.1. Relationship between fibrin accumulation and foreign body reactions

To investigate foreign body reactions to particle implants, $TiO_2$ (50 μL, 10% w/v), PLA particles (50 μL, 10% w/v), and saline (100 μL) were injected subcutaneously. One day after implantation, tissue samples were harvested and then analyzed histologically. By analyzing implants and surrounding tissue, we found that both $TiO_2$ and PLA sites had a large amount of fibrin accumulation. The relative amount of fibrin at the $TiO_2$ implantation sites however, was considerably more than that at the PLA sites (Fig. 1A). Furthermore, saline controls had very low or no fibrin accumulation during the same time period. By quantifying the inflammatory cells and fibrin amounts, we found a good relationship between the relative amount of fibrin and the inflammatory cell recruitment (Fig. 1B). These results reveal that fibrin deposition may serve as a viable early indicator of foreign body reactions.

### 3.2. Properties of the fibrin-affinity probes

For real-time monitoring of fibrin accumulation *in vivo*, an imaging probe was fabricated by direct conjugation between fibrinaffinity peptide and NIR dye. Fluorescence spectroscopic results demonstrated that the fibrin-affinity probes have a fluorescence spectrum with a maximum emission at 812 nm at an excitation of 796 nm (Fig. 2A). The cytotoxicity of the fibrin-affinity probes was determined using 3T3 fibroblasts and an MTS assay (Fig. 2B). We found that the fibrin-affinity probes trigger no statistically significant cytotoxicity over the

studied concentration range (up to 0.35 μg/mL), indicating that the above probes possess adequate cell compatibility for further *in vivo* testing.

### 3.3. In vitro fibrin targeting of the fibrin-affinity probe

The ability of the fibrin-affinity probe to detect fibrin deposition was evaluated using fibrin-coated glass beads. After incubation with fibrin-affinity probes (GPRPPGGSKGC-Oyster800) or its control (Oyster800), the glass beads were observed under an optical microscope. As expected, the fluorescence signal at the fibrin sites [shown in red (in web version)] was very high (fluorescence intensity = 81.95). However, there was almost no control probe accumulation in the fibrin area (fluorescence intensity = 31.96, Fig. 2C). These findings support the hypothesis that fibrin-affinity probes may be used to specifically detect the presence of fibrin. To further study whether the probes can be used to quantify the amounts of fibrin *in vitro*, the probes were incubated with glass beads coated with various amounts of fibrin, and the fibrin-associated fluorescence intensities were determined. In support of the hypothesis, a good linear relationship was found between fibrin amount and fluorescence intensities in the fibrin probe group. In contrast, the fluorescence intensities associated with the control group was approximately equal to the background (Fig. 2D). Overall, the *in vitro* results support that fibrin-affinity probes can preferentially bind to fibrin and may be used to quantify the amount of fibrin *in vitro*.

### 3.4. Detection of fibrin accumulation in vivo using fibrin-affinity probes

First, to evaluate whether fibrin-affinity probes can be used specifically to assess the deposition of fibrin *in vivo*, thrombin (25 U) and saline, as a control, were injected subcutaneously. Following the subcutaneous injection, 60 μL of the fibrin-affinity probe (0.5 mg/mL) was administrated intravenously. It is well known that thrombin can cleave fibrinogen, prompting its polymerization and thus fibrin formation [9]. We found that within 30 min of thrombin injection, the fibrin probe accumulated around the implantation sites. Fluorescence signals were observed to increase over time, and the signal intensity around the thrombin implantation sites was consistently higher than that in the saline control sites (Fig. 2E).

The effectiveness of fibrin-affinity probes for detecting fibrin deposition at biomaterial implant sites was then tested *in vivo*. $TiO_2$ (10 mg/50 μL) was administered subcutaneously on the back of mice prior to intravascular administration of a 60 μL fibrin-affinity probe solution (0.5 mg/mL). Following the fibrin-affinity probe injection, whole body images were recorded at different time points (Fig. 3A). A substantial increase in fluorescence intensity was found at the $TiO_2$ injection site, in as short as 10 min following probe injection, in comparison to the saline control. The accumulation of the fibrin-affinity probe at the $TiO_2$ site increased with time and reached its plateau around 1 h, where the $TiO_2$ treatment triggered ~16 times higher fluorescence intensity than the saline control (Fig. 3A).

To confirm that the accumulation of the fibrin-affinity probe was mediated by localized fibrin deposition, control studies were carried out in which animals were implanted with $TiO_2$ nanospheres in the presence or absence of anti-coagulant – heparin (10 U/site). Many studies have shown that heparin can prevent the formation of a stable fibrin clot in inhibiting the activation of the fibrin stabilizing factor [30,31]. The probes were subsequently administered intravenously and images were captured 1 h after the probe injection. As expected, treatment with heparin substantially reduced the accumulation of the fibrin-affinity probe by about 2 fold at the implantation site (Fig. 3B and C). These results showed that the fibrin-affinity probes may be used to non-invasively monitor fibrin deposition at the implant sites. Since there is a good relationship between fibrin deposition and inflammatory

responses, it is likely that fibrin-affinity can also be used as a tool for the early detection of foreign body reactions.

### 3.5. Effect of mast cells on fibrin deposition using fibrin-affinity probes

Many previous studies have shown that mast cell activation is essential for fibrin accumulation in different inflammatory diseases. We thus hypothesize that mast cell activation is responsible for fibrin deposition surrounding biomaterial implants. To test this hypothesis, we investigated fibrin accumulation in mice treated with mast cell activator, compound 48/80 (100 μg/site), or saline [32]. As expected, the fluorescence signal at compound 48/80 sites was approximately 16 folds higher than the saline control site (Fig. 4A). By quantifying fibrin densities from histological staining, we also found abundant amounts of fibrin accumulation at compound 48/80 implantation sites, with less fibrin accumulation at saline sites (Fig. 4B). To determine the relationship between fibrin-affinity probe accumulation and implant-mediated fibrin density, we correlated both the fibrin densities with the fluorescence intensity. Our results show strong linear trends between the fibrin densities and the fluorescence intensity (Fig. 4C).

### 3.6. Quantification of inflammatory reactions induced by different types of implants

Subsequent studies were carried out to explore the possibility of using fibrin-affinity probes to assess inflammatory reactions to different biomaterial implants *in vivo*. $TiO_2$, $SiO_2$ and PLA particles were chosen as model materials which have been shown to trigger strong and weak inflammatory responses [33,34]. After material implantation for 15 min, the implant sites were first imaged. We found that, in the absence of probes, there was no false signal from the control groups (Fig. S1). On the other hand, 1 h after administration of the fibrin-affinity probe, various extents of probe-associated fluorescent intensities were found at the sites of particle implantation in the order: $TiO_2$ > PLA > $SiO_2$ (Fig. 5A). By correlating imaging results and fibrin densities from histological staining, we found that there is a very good relationship between implant-associated fibrin-affinity probe accumulation and localized fibrin deposition (Fig. 5B). These results confirm that the fibrin-affinity probes may be used to quantify the extent of implant-mediated fibrin deposition at the implant sites. The extent of the inflammatory response associated with 4 day implants was also examined by histological staining (Fig. 5C). The total inflammatory cell numbers of the three materials were also calculated from CD11b+ staining. In agreement with previous findings, we found a positive linear relationship between fluorescence intensity from fibrin probes and total inflammatory cell numbers from CD11b+ staining ($R^2$ = 0.84). This demonstrates that these fibrin probes can be used for early prediction of foreign body reactions.

To confirm the role of mast cells in implant-mediated fibrin deposition, we used mast cell-deficient (WBB6F1-W/$W^v$) mice and their normal littermates (WBB6F1-+/+). A number of earlier investigations have shown these mice to be valuable tools for determination of mast cell functions *in vivo* [12,15]. Interestingly, the fluorescence intensities of different particles in the mast cell-deficient mice, WBB6F1-W/$W^v$ (W/$W^v$), dramatically decreased (~48% at $TiO_2$, ~52% at $SiO_2$, and ~44% at PLA) compared to the normal littermates (Fig. 5D). These results support that mast cell activation is responsible for fibrin deposition surrounding biomaterial implants.

## 4. Discussion

Many imaging probes have been developed to monitor different cells and processes of foreign body reactions [27,28,35–37]. However, to the best of our knowledge, no real-time imaging tool has been developed to detect mast cell responses. Since mast cell activation is responsible for early fibrin deposition at the inflamed sites [11,12,15] and inflammatory cell

recruitment to the implanted biomaterials [38,39], it is likely that the early detection of fibrin deposition may predict the extent of subsequent/long-term inflammatory cell recruitment and in-flammatory/fibrotic tissue responses. This hypothesis is supported by many early observations. Excessive generation of fibrin is always accompanied by the recruitment and activation of inflammatory cells, leading to an increased inflammatory response [40–42]. Many studies have also documented that extravascular fibrin deposition can be an early and persistent hallmark of inflammatory responses and foreign body reactions [3,4].

In the present study, GPRPPGGSKGC was selected as a fibrin(ogen) targeting peptide based on the following advantages. First, the tri-peptide, Gly–Pro–Arg, has been shown to inhibit the clotting of fibrin and thrombin because it consists of the N-terminal sequence of the α-chain of fibrin [23]. Further studies have identified the peptide Gly–Pro–Arg–Pro–Pro (GPRPP) as a highly avid fibrin-affinity agent possessing increased resistance to proteolysis [22,24]. In this study, a fibrin-affinity probe was fabricated by conjugating fibrin-affinity peptides (GPRPPGGSKGC) and Oyster800 dye. Oyster-800 dye was chosen because of its biocompatibility and high wavelength (~800 nm) with minimal tissue absorbance and background for improved fluorescence sensitivity during *in vivo* imaging [21,27,28]. By direct conjugation of the peptide with NIR dye, we substantially reduced the size of our probe. This makes it a suitable vehicle to detect the accumulation of fibrin *in vivo*, especially since fibrin clots always occur in the injury/inflammation sites in proximity to the blood stream [43,44]. Indeed, our results have shown that substantial accumulation of fibrin-affinity probes occurs at the implant sites around 10 min and achieves a plateau at 1 h following probe administration and material implantation. Many studies have demonstrated that inactive fibrinogen can convert into fibrin by thrombin injection [26,45]. In a similar manner, our results show that the fibrin-affinity probes accumulate in the area of thrombin-induced fibrin deposition immediately following intravenous injection, which is consistent with previous findings that used thrombin-induced fibrin deposition [46]. Subcutaneous injection of particles ($TiO_2$) is a well-established inflammation model prompting a foreign body response accompanied by fibrin deposition [33,34]. Indeed, immediately following intravenous injection, fibrin-affinity probes accumulate in the area of $TiO_2$-induced inflammation. Additionally, the substantial reduction of probe accumulation in mice following an anti-coagulant treatment further supports the fact that this fibrin-affinity probe can target the accumulation of fibrin at the inflamed sites. Furthermore, the ability of the fibrin-affinity probes to detect and quantify foreign body reactions was tested using different materials. It is well documented that different biomaterial implants can prompt varying inflammatory responses [47]. By implanting various biomaterials ($TiO_2$, $SiO_2$, PLA), it has been confirmed that our fibrin-affinity probes can be used to image and assess the extent of fibrin deposition at particle implantation sites.

Many early studies have shown that mast cells are responsible for fibrin deposition in many inflammatory diseases [12]. Although previous studies have demonstrated that histamine release and mast cell activation are both important to the early-phase foreign body reaction [4,15], the role of mast cell activation on fibrin deposition around biomaterial implants has not yet been determined. Thus, a series of studies were carried out to elucidate mast cell participation in fibrin deposition during foreign body responses. First, by localized activation of mast cells via c48/80 administration [15,48], we found >10 fold increase in the fibrin-affinity probe accumulation at treatment sites as compared with saline controls. The role of mast cells in implant-mediated fibrin deposition was further tested using mast cell-deficient WBB6F1-W/$W^v$ (W/$W^v$) mice and their normal littermates, WBB6F1-+/+ (+/+). As expected, we found that the accumulation of fibrin-affinity probes at the implant sites was substantially reduced in mast cell-deficient (W/$W^v$) mice (~48% at $TiO_2$, ~52% at $SiO_2$, and ~44% at PLA) in comparison with the normal littermates (+/+). The results indicate that mast cells may play a significant regulatory role in fibrin deposition during biomaterial-

induced foreign body responses, which is in agreement with previous findings [15]. It should be noted that the probe may affect fibrin deposition, since triple peptide Gly–Pro–Arg in this probe has been shown to inhibit fibrin polymerization. Fortunately, only a small quantity of the peptide is needed for probe fabrication and only a small amount of probes are needed for *in vivo* detection. Finally, our results have shown that the administration of the fibrin probe did not alter the relative extent of host responses to particle implants.

Overall, this study demonstrates that fibrin-affinity probes can be fabricated to specifically detect fibrin deposition in real time *in vivo*. Since fibrin deposition represents an early stage of inflammatory responses, mast cell activation is essential to fibrin accumulation in tissue. Our results suggest that fibrin-affinity probes may provide a rapid assessment of biomaterials' tissue compatibility. Additionally, we can also use fibrin-affinity probes to evaluate the extent of mast cell activation reflected by the degree of fibrin deposition surrounding biomaterial implants. Finally, this information would greatly improve the understanding of the processes of fibrin deposition and mast cell participation in the foreign body response to biomaterials.

## 5. Conclusions

Taking advantage of the high affinity of peptide GPRPPGGSKGC to fibrin(ogen), a fibrin-affinity NIR probe was developed to detect the accumulation of fibrin. The probes were found to have a high affinity and specificity for fibrin deposition *in vitro*. In addition, the fibrin probe can be used to assess the extent of implant-associated fibrin deposition. Further studies suggest that mast cell activation is responsible for fibrin deposition in implant surrounding tissues. These results demonstrate that the fibrin-affinity probe may be used as a quick, non-invasive, *in vivo* imaging tool for real-time evaluation of fibrin deposition, mast cell activation, and foreign body responses.

## Supplementary Material

Refer to Web version on PubMed Central for supplementary material.

## Acknowledgments

This work was supported by an NIH grant R43 GM101776.

## References

1. Hu WJ, Eaton JW, Ugarova TP, Tang L. Molecular basis of biomaterial-mediated foreign body reactions. Blood. 2001; 98:1231–8.
2. Tang L, Eaton JW. Natural responses to unnatural materials: a molecular mechanism for foreign body reactions. Mol Med. 1999; 5:351–8. [PubMed: 10415159]
3. Smiley ST, King JA, Hancock WW. Fibrinogen stimulates macrophage chemokine secretion through toll-like receptor 4. J Immunol. 2001; 167:2887–94.
4. Tang L, Eaton JW. Fibrin(ogen) mediates acute inflammatory responses to biomaterials. J Exp Med. 1993; 178:2147–56.
5. Languino LR, Plescia J, Duperray A, Brian AA, Plow EF, Geltosky JE, et al. Fibrinogen mediates leukocyte adhesion to vascular endothelium through an icam-1-dependent pathway. Cell. 1993; 73:1423–34.
6. Altieri DC, Bader R, Mannucci PM, Edgington TS. Oligospecificity of the cellular adhesion receptor mac-1 encompasses an inducible recognition specificity for fibrinogen. J Cell Biol. 1988; 107:1893–900. [PubMed: 3053736]

7. Loike JD, Sodeik B, Cao L, Leucona S, Weitz JI, Detmers PA, et al. Cd11c/cd18 on neutrophils recognizes a domain at the n terminus of the a alpha chain of fibrinogen. Proc Natl Acad Sci U S A. 1991; 88:1044–8. [PubMed: 1671533]
8. Perez RL, Roman J. Fibrin enhances the expression of IL-1 beta by human peripheral blood mononuclear cells: implications in pulmonary inflammation. J Immunol. 1995; 154:1879–87. [PubMed: 7836771]
9. Szaba FM, Smiley ST. Roles for thrombin and fibrin(ogen) in cytokine/chemokine production and macrophage adhesion in vivo. Blood. 2002; 99:1053–9.
10. Akassoglou K, Adams RA, Bauer J, Mercado P, Tseveleki V, Lassmann H, et al. Fibrin depletion decreases inflammation and delays the onset of demyelination in a tumor necrosis factor transgenic mouse model for multiple sclerosis. Proc Natl Acad Sci U S A. 2004; 101:6698–703.
11. Valent P, Sillaber C, Baghestanian M, Bankl HC, Kiener HP, Lechner K, et al. What have mast cells to do with edema formation, the consecutive repair and fibrinolysis? Int Arch Allergy Immunol. 1998; 115:2–8. [PubMed: 9430489]
12. Ramos BF, Zhang Y, Jakschik BA. Mast cells contribute to fibrin deposition in reverse passive arthus reaction in mouse skin. Eur J Immunol. 1992; 22:2381–5.
13. Tang L, Ugarova TP, Plow EF, Eaton JW. Molecular determinants of acute in-flammatory responses to biomaterials. J Clin Invest. 1996; 97:1329–34. [PubMed: 8636446]
14. Zdolsek J, Eaton JW, Tang L. Histamine release and fibrinogen adsorption mediate acute inflammatory responses to biomaterial implants in humans. J Transl Med. 2007; 5:31.
15. Tang L, Jennings TA, Eaton JW. Mast cells mediate acute inflammatory responses to implanted biomaterials. Proc Natl Acad Sci U S A. 1998; 95:8841–6.
16. Pan D, Caruthers SD, Hu G, Senpan A, Scott MJ, Gaffney PJ, et al. Ligand-directed nanobialys as theranostic agent for drug delivery and manganese-based magnetic resonance imaging of vascular targets. J Am Chem Soc. 2008; 130:9186–7. [PubMed: 18572935]
17. McCarthy JR, Patel P, Botnaru I, Haghayeghi P, Weissleder R, Jaffer FA. Multimodal nanoagents for the detection of intravascular thrombi. Bioconjug Chem. 2009; 20:1251–5. [PubMed: 19456115]
18. Botnar RM, Perez AS, Witte S, Wiethoff AJ, Laredo J, Hamilton J, et al. In vivo molecular imaging of acute and subacute thrombosis using a fibrin-binding magnetic resonance imaging contrast agent. Circulation. 2004; 109:2023–9.
19. Overoye-Chan K, Koerner S, Looby RJ, Kolodziej AF, Zech SG, Deng Q, et al. EP-2104R: a fibrin-specific gadolinium-based MRI contrast agent for detection of thrombus. J Am Chem Soc. 2008; 130:6025–39.
20. Pan D, Senpan A, Caruthers SD, Williams TA, Scott MJ, Gaffney PJ, et al. Sensitive and efficient detection of thrombus with fibrin-specific manganese nanocolloids. Chem Commun. 2009:3234–6.
21. Frangioni JV. In vivo near-infrared fluorescence imaging. Curr Opin Chem Biol. 2003; 7:626–34. [PubMed: 14580568]
22. Aruva MR, Daviau J, Sharma SS, Thakur ML. Imaging thromboembolism with fibrin-avid 99mTc-peptide: evaluation in swine. J Nucl Med. 2006; 47:155–62.
23. Laudano AP, Doolittle RF. Synthetic peptide derivatives that bind to fibrinogen and prevent the polymerization of fibrin monomers. Proc Natl Acad Sci U S A. 1978; 75:3085–9.
24. Thakur ML, Pallela VR, Consigny PM, Rao PS, Vessileva-Belnikolovska D, Shi R. Imaging vascular thrombosis with 99mTc-labeled fibrin alpha-chain peptide. J Nucl Med. 2000; 41:161–8.
25. Sohaebuddin SK, Thevenot PT, Baker D, Eaton JW, Tang L. Nanomaterial cytotoxicity is composition, size, and cell type dependent. Part Fibre Toxicol. 2010; 7:22.
26. Neeves KB, Illing DA, Diamond SL. Thrombin flux and wall shear rate regulate fibrin fiber deposition state during polymerization under flow. Biophys J. 2010; 98:1344–52. [PubMed: 20371335]
27. Zhou J, Tsai YT, Weng H, Tang EN, Nair A, Dave DP, et al. Real-time detection of implant-associated neutrophil responses using a formyl peptide receptor-targeting NIR nanoprobe. Int J Nanomed. 2012; 7:2057–68.

28. Zhou J, Tsai YT, Weng H, Baker DW, Tang L. Real time monitoring of biomaterial-mediated inflammatory responses via macrophage-targeting NIR nanoprobes. Biomaterials. 2011; 32:9383–90.
29. Gray LD, Hussey MA, Larson BM, Machlus KR, Campbell RA, Koch G, et al. Recombinant factor VIIa analog NN1731 (V158D/E296V/M298Q-FVIIa) enhances fibrin formation, structure and stability in lipidated hemophilic plasma. Thromb Res. 2011; 128:570–6.
30. Hogg PJ, Jackson CM, Labanowski JK, Bock PE. Binding of fibrin monomer and heparin to thrombin in a ternary complex alters the environment of the thrombin catalytic site, reduces affinity for hirudin, and inhibits cleavage of fibrinogen. J Biol Chem. 1996; 271:26088–95.
31. Simmons CA, Burdick MD, Schaub RG. Heparin inhibits fibrin, but not leukocytes, in a model of deep-vein thrombosis. J Surg Res. 1987; 43:468–75. [PubMed: 3682807]
32. Zhou J, Tsai YT, Weng H, Tang L. Noninvasive assessment of localized in-flammatory responses. Free Radic Biol Med. 2012; 52:218–26. [PubMed: 22080048]
33. Dorozhkin SV. Biocomposites and hybrid biomaterials based on calcium orthophosphates. Biomatter. 2011; 1:3–56. [PubMed: 23507726]
34. Kokubo T, Kim HM, Kawashita M. Novel bioactive materials with different mechanical properties. Biomaterials. 2003; 24:2161–75. [PubMed: 12699652]
35. Bratlie KM, Dang TT, Lyle S, Nahrendorf M, Weissleder R, Langer R, et al. Rapid biocompatibility analysis of materials via in vivo fluorescence imaging of mouse models. PLoS One. 2010; 5:e10032. [PubMed: 20386609]
36. Ma M, Liu WF, Hill PS, Bratlie KM, Siegwart DJ, Chin J, et al. Development of cationic polymer coatings to regulate foreign-body responses. Adv Mater. 2011; 23:H189–94. [PubMed: 21567481]
37. Liu WF, Ma M, Bratlie KM, Dang TT, Langer R, Anderson DG. Real-time in vivo detection of biomaterial-induced reactive oxygen species. Biomaterials. 2011; 32:1796–801.
38. Anderson JM, Rodriguez A, Chang DT. Foreign body reaction to biomaterials. Semin Immunol. 2008; 20:86–100.
39. Coleman JW. Nitric oxide: a regulator of mast cell activation and mast cell-mediated inflammation. Clin Exp Immunol. 2002; 129:4–10.
40. van Hinsbergh VW, Collen A, Koolwijk P. Role of fibrin matrix in angiogenesis. Ann N Y Acad Sci. 2001; 936:426–37.
41. Pereira M, Simpson-Haidaris PJ. Fibrinogen modulates gene expression in wounded fibroblasts. Ann N Y Acad Sci. 2001; 936:438–43. [PubMed: 11460497]
42. Simpson-Haidaris PJ, Rybarczyk B. Tumors and fibrinogen: the role of fibrinogen as an extracellular matrix protein. Ann N Y Acad Sci. 2001; 936:406–25.
43. Andre P, Hartwell D, Hrachovinova I, Saffaripour S, Wagner DD. Pro-coagulant state resulting from high levels of soluble p-selectin in blood. Proc Natl Acad Sci U S A. 2000; 97:13835–40.
44. Cooley BC. In vivo fluorescence imaging of large-vessel thrombosis in mice. Arterioscler Thromb Vasc Biol. 2011; 31:1351–6.
45. Aspenberg P, Virchenko O. Platelet concentrate injection improves achilles tendon repair in rats. Acta Orthop Scand. 2004; 75:93–9.
46. Gomi K, Zushi M, Honda G, Kawahara S, Matsuzaki O, Kanabayashi T, et al. Antithrombotic effect of recombinant human thrombomodulin on thrombin-induced thromboembolism in mice. Blood. 1990; 75:1396–9.
47. Tang L, Hu W. Molecular determinants of biocompatibility. Expert Rev Med Dev. 2005; 2:493–500.
48. Metz M, Maurer M. Mast cellsekey effector cells in immune responses. Trends Immunol. 2007; 28:234–41.

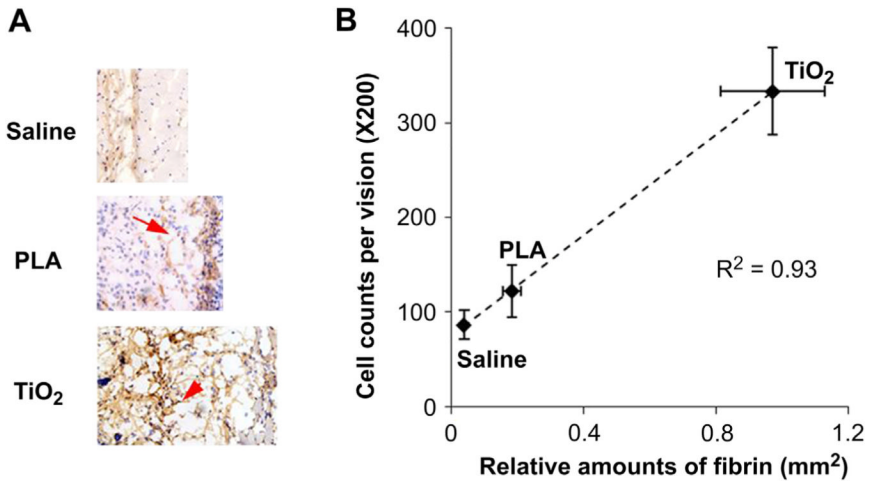


**Fig. 1.**

Relationship between fibrin accumulation and the recruitment of inflammatory cells. (A) Representative fibrin examination of the tissue surrounding $TiO_2$, PLA and saline implants; (B) The relationship between relative fibrin density and inflammatory cell counts. Mice were sacrificed and tissue samples were collected one day after particle implantation.

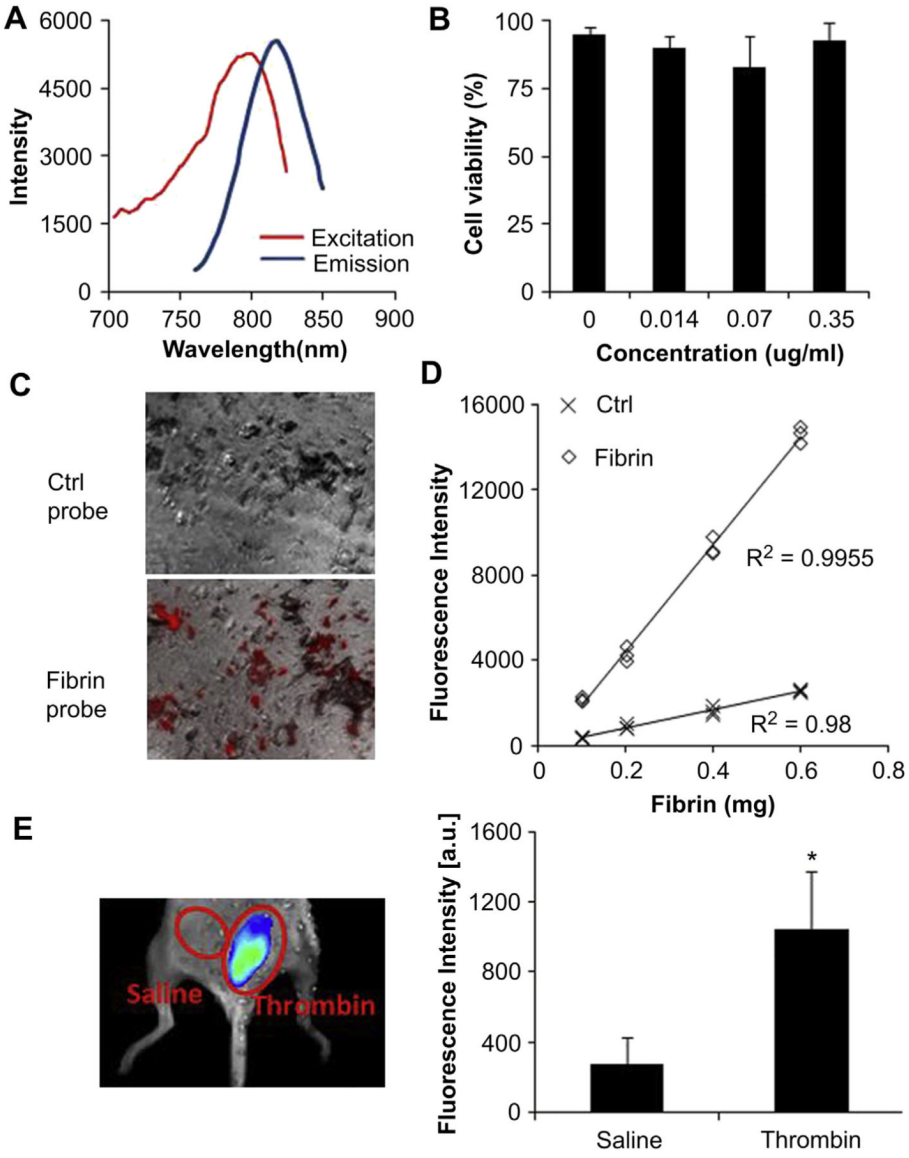


**Fig. 2.**

Characterization of fibrin-affinity probes and assessment of the specificity of fibrin *in vitro* and *in vivo*. (A) Excitation and emission spectra of fibrin-affinity probes (B) Cytotoxicity study of fibrin-affinity probes using an MTS assay. (C) Fluorescence microscopy images of fibrin clots on the glass beads incubated with fibrin-affinity probes and control probes (red color represents the probe). (D) Correlation between fibrin amounts and fluorescence intensities following incubation with either fibrin-affinity probes or control probes. (E) The merged fluorescence and white light images (left panel) show the accumulation of the fibrin-affinity probes at thrombin injection sites, but not the control site (saline injection). The mean fluorescence intensities at thrombin injection sites and saline injection sites (right panel); Bars represent the mean of four mice, error bars represent standard deviation (s.d.), * denotes $p < 0.05$. (For interpretation of the references to color in this figure legend, the reader is referred to the web version of this article.)

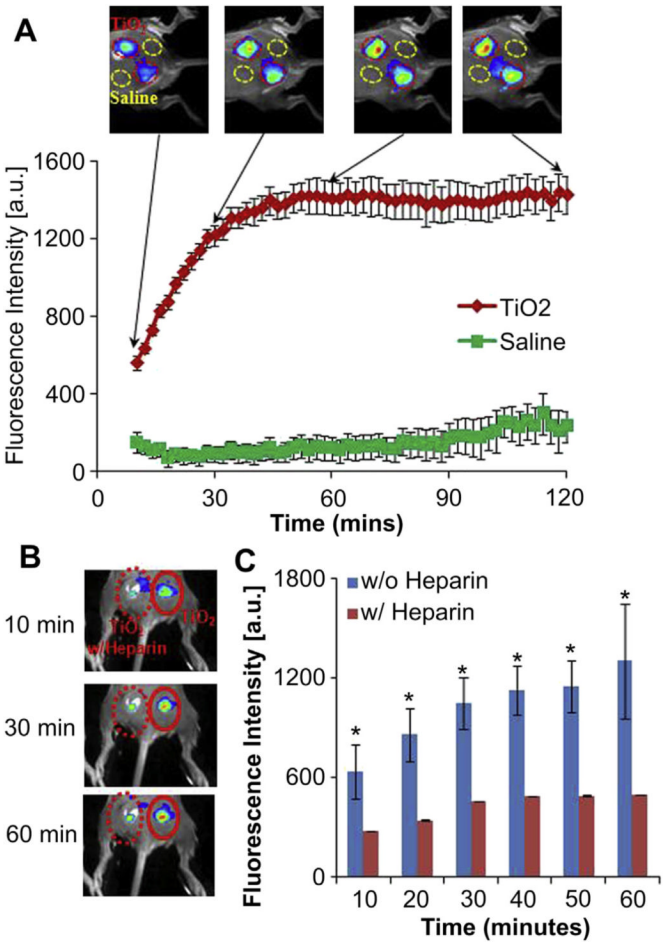


**Fig. 3.**

(A) The merged fluorescence and white light images (top panel) show the accumulation of fibrin-affinity probes at the $TiO_2$ injection sites, but not the control site (saline injection). The mean fluorescence intensities at the $TiO_2$ injection sites, but not saline injection sites, increased with time (bottom panel). (B) *In vivo* fluorescence imaging post-injection illustrates the diminishing accumulation of fibrin-affinity probes around $TiO_2$ with heparin treatment in comparison with $TiO_2$ alone within 1 h. (C) Quantification of fluorescence intensities within 1 h. Each mouse in test groups ($n = 4$) was treated with the probe (60 μL, 0.5 mg/mL). Error bars represent standard deviation (s.d.), * denotes $p < 0.05$. (For interpretation of the references to color in this figure legend, the reader is referred to the web version of this article.)

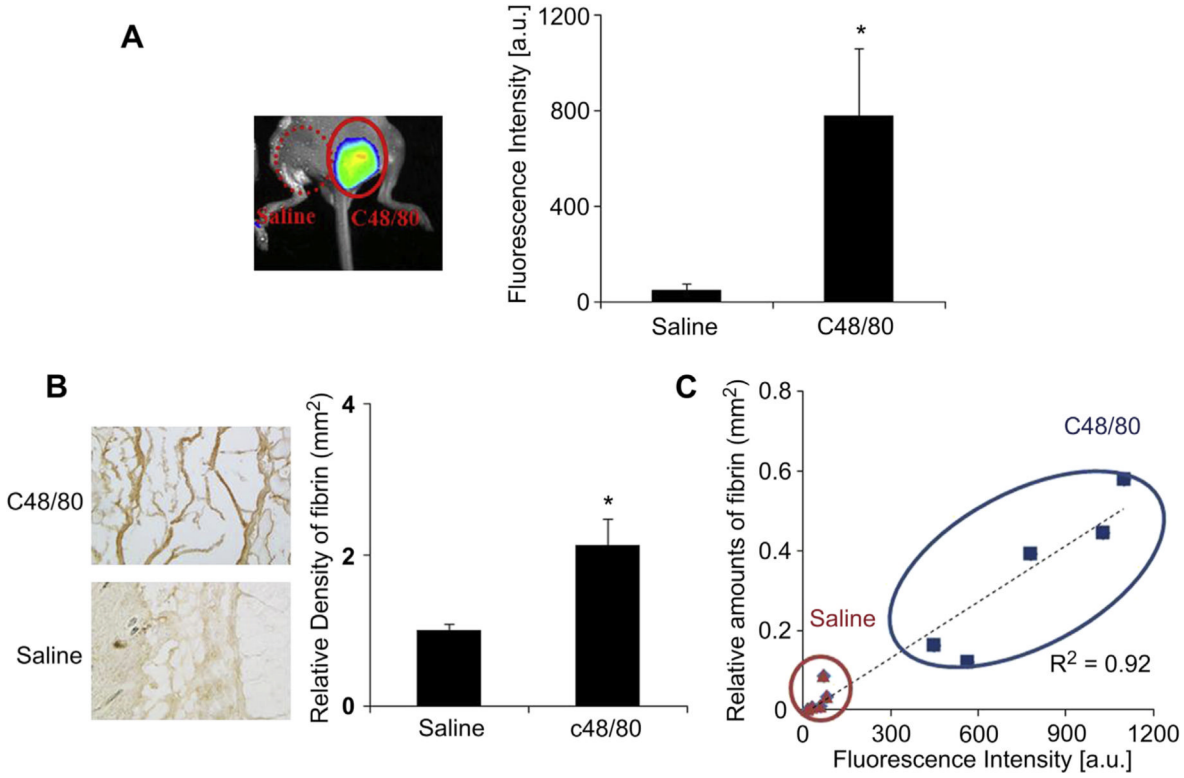


**Fig. 4.**

To evaluate mast cell activation using fibrin-affinity probe injection, mice were subcutaneously injected with 100 mg of c48/80 or saline as a control. Immediately after injection, probe (60 μL, 0.5 mg/mL) was administered retro-orbital injection. Imaging was captured 4 h after probe administration. Animals were subsequently sacrificed and tissue samples were harvested for histological analysis. (A) Representative in vivo fluorescence imaging (left) and quantitative analysis (right) of the fluorescence intensity at c48/80 and saline control sites. (B) Representative fibrin examination of the tissue surrounding c48/80 and saline control sites. (C) Correlation between relative fibrin accumulation and fibrin-affinity probe associated fluorescent intensities at c48/80 and saline control sites. Four mice were used in the experiments. Error bars represent standard deviation (s.d.), * denotes $p < 0.05$. (For interpretation of the references to color in this figure legend, the reader is referred to the web version of this article.)

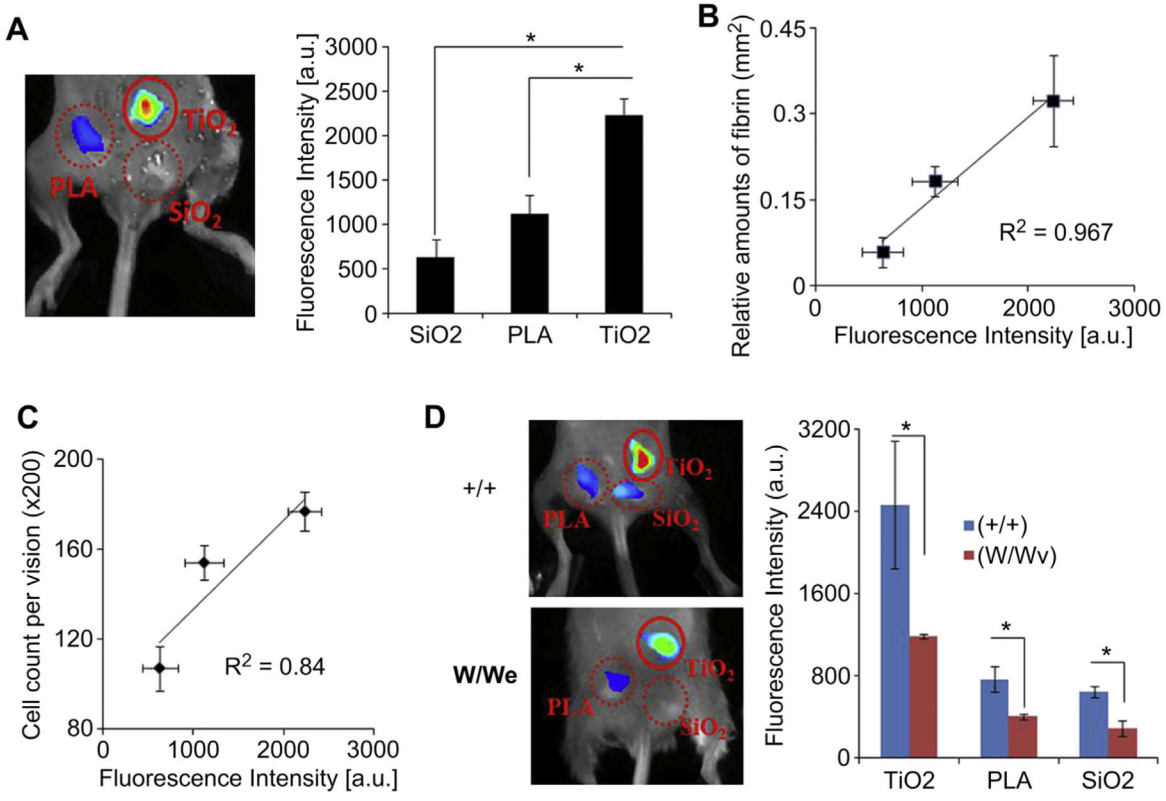


**Fig. 5.**

In a foreign body response animal model, $TiO_2$, $SiO_2$, and PLA were implanted subcutaneously in the back of mice ($n = 3$). The probe was administered 10 min after implantation. The animal images were taken after 1 h, animals were sacrificed and tissue samples were harvested for histological analysis. (A) Representative *in vivo* fluorescence imaging (left) and quantitative analysis (right) of the fluorescence intensity at different implantation sites ($TiO_2$, $SiO_2$, PLA). (B) Correlation between relative fibrin accumulation and fibrin-affinity probe associated fluorescent intensities at different implantation sites. (C) Correlation between inflammatory cell counts from CD11b+ staining and fibrin-affinity probe associated fluorescent intensities at different implantation sites. (D) *In vivo* image (left panel) and fluorescence intensities (right panel) illustrate the diminishing accumulation of fibrin-affinity probes in mast cell deficiency ($W/W^v$) mice ($n = 3$) in comparison with wild type (+/+) ($n = 3$). Error bars represent standard deviation (s.d.), * denotes $p < 0.05$. (For interpretation of the references to color in this figure legend, the reader is referred to the web version of this article.)